nature climate change

LETTERS

PUBLISHED ONLINE: 23 FEBRUARY 2015 | DOI: 10.1038/NCLIMATE2541

Climatic and biotic thresholds of coral-reef shutdown

Lauren T. Toth[1*†], Richard B. Aronson[1,2], Kim M. Cobb[3], Hai Cheng[4,5], R. Lawrence Edwards[5], Pamela R. Grothe[3] and Hussein R. Sayani[3]

Climate change is now the leading cause of coral-reef degradation and is altering the adaptive landscape of coral populations[1,2]. Increasing sea temperatures and declining carbonate saturation states are inhibiting short-term rates of coral calcification, carbonate precipitation and submarine cementation[3–5]. A critical challenge to coral-reef conservation is understanding the mechanisms by which environmental perturbations scale up to influence long-term rates of reef-framework construction and ecosystem function[6,7]. Here we reconstruct climatic and oceanographic variability using corals sampled from a 6,750-year core from Pacific Panamá. Simultaneous reconstructions of coral palaeophysiology and reef accretion allowed us to identify the climatic and biotic thresholds associated with a 2,500-year hiatus in vertical accretion beginning ~4,100 years ago[8]. Stronger upwelling, cooler sea temperatures and greater precipitation—indicators of La Niña-like conditions—were closely associated with abrupt reef shutdown. The physiological condition of the corals deteriorated at the onset of the hiatus, corroborating theoretical predictions that the tipping points of radical ecosystem transitions should be manifested sublethally in the biotic constituents[9]. Future climate change could cause similar threshold behaviours, leading to another shutdown in reef development in the tropical eastern Pacific.

Climatic and oceanographic variability have played a dominant role in the development of reefs throughout the Phanerozoic eon[10], and the recent past is no exception. In Panamá and several other locations in the Pacific, coral reefs stopped accreting vertically for 2,500 years, beginning ~4,100 cal yr BP (ref. 8; calibrated ^{14}C calendar years before 1950; Fig. 1a). Correlations with regional palaeoclimate proxies suggest that enhanced variability of the El Niño/Southern Oscillation (ENSO) was the ultimate cause of reef shutdown in the tropical eastern Pacific[8] (TEP). Climatic shifts at that time led to environmental and cultural impacts on a global scale[11,12].

In this study we investigated the long-term impacts of environmental variability on coral physiology and reef development in the TEP to ascertain the climatic, oceanographic and biotic controls on ecosystem state in the past. We quantified the range of environmental conditions that corals experienced during the past ~6,750 years to determine whether significant changes in climate or oceanography were associated with changes in coral physiology or reef accretion. We then evaluated the environmental and physiological thresholds that characterized the catastrophic phase shift to the hiatus.

In Pacific Panamá, El Niño-like periods are characterized by a warm, dry climate and a reduction in seasonal upwelling. Those conditions are reversed during La Niña-like periods (Supplementary Discussion and Supplementary Fig. 1). Contemporary environmental variability is high at Contadora Island, a site in Pacific Panamá that is exposed to intense seasonal upwelling and the interannual impacts of ENSO. We extracted a 2.68-m, vertical push-core, designated EP09-28, from the uncemented reef framework at Contadora. The framework is built of branch fragments of *Pocillopora* spp. corals packed in fine sediment (Supplementary Fig. 3). Through geochemical analysis of the coral skeletons, we reconstructed reef palaeoenvironments and changes in coral physiology during the entire Holocene history of the Contadora reef, from its initiation ~6,750 cal yr BP to present (Supplementary Table 4 and Supplementary Fig. 7).

To constrain environmental conditions before and after the hiatus we measured the elemental ratios and isotopic compositions of 133 diagenetically unaltered *Pocillopora* skeletons distributed throughout the core (Supplementary Fig. 4). Our palaeoclimatic reconstructions are based on temperature calibrations for Sr/Ca and oxygen isotopes (δ^{18}O) using modern *Pocillopora damicornis* colonies from Contadora (Fig. 2 and Supplementary Figs 5 and 6). Whereas Sr/Ca in coral skeletons is primarily driven by temperature, δ^{18}O reflects a combination of temperature and seawater δ^{18}O ($\delta^{18}O_{sw}$), which generally tracks hydrologic variability[13] (Fig. 2). We identified a significant relationship between Sr/Ca and temperature (Fig. 2a), and between coral-reconstructed $\delta^{18}O_{sw}$ and local precipitation (Fig. 2c), in the modern corals. The modern-day calibration confirmed that Sr/Ca and δ^{18}O records from pocilloporid corals capture the seasonal range in climate characterized by intense winter-time upwelling of cooler water (high Sr/Ca and high δ^{18}O) accompanied by dry conditions (high $\delta^{18}O_{sw}$).

At each sampled horizon in the core, we used multiple coral fragments to reconstruct: palaeotemperature and palaeosalinity from Sr/Ca and δ^{18}O (ref. 13); oceanic palaeoproductivity (upwelling), primarily from the local reservoir correction ΔR ($= \Delta^{14}C$; ref. 8; Supplementary Methods) and to a lesser extent from Ba/Ca (ref. 14); and coral physiology from δ^{13}C and B/Ca (refs 15–18). Although there has been much debate over the interpretation of δ^{13}C in coral skeletons, its variability is generally assumed to be driven by metabolic processes in the

[1]Department of Biological Sciences, Florida Institute of Technology, Melbourne, Florida 32901, USA. [2]Smithsonian Marine Station and National Museum of Natural History, Smithsonian Institution, Washington DC 20560, USA. [3]Department of Earth and Atmospheric Sciences, Georgia Institute of Technology, Atlanta, Georgia 30332, USA. [4]Institute of Global Environmental Change, Xi'an Jiaotong University, Xi'an 710049, China. [5]Department of Earth Sciences, University of Minnesota, Minneapolis, Minnesota 55455, USA. †Present address: US Geological Survey, Coastal and Marine Science Center, St Petersburg, Florida 33701, USA. *e-mail: ltoth@usgs.gov

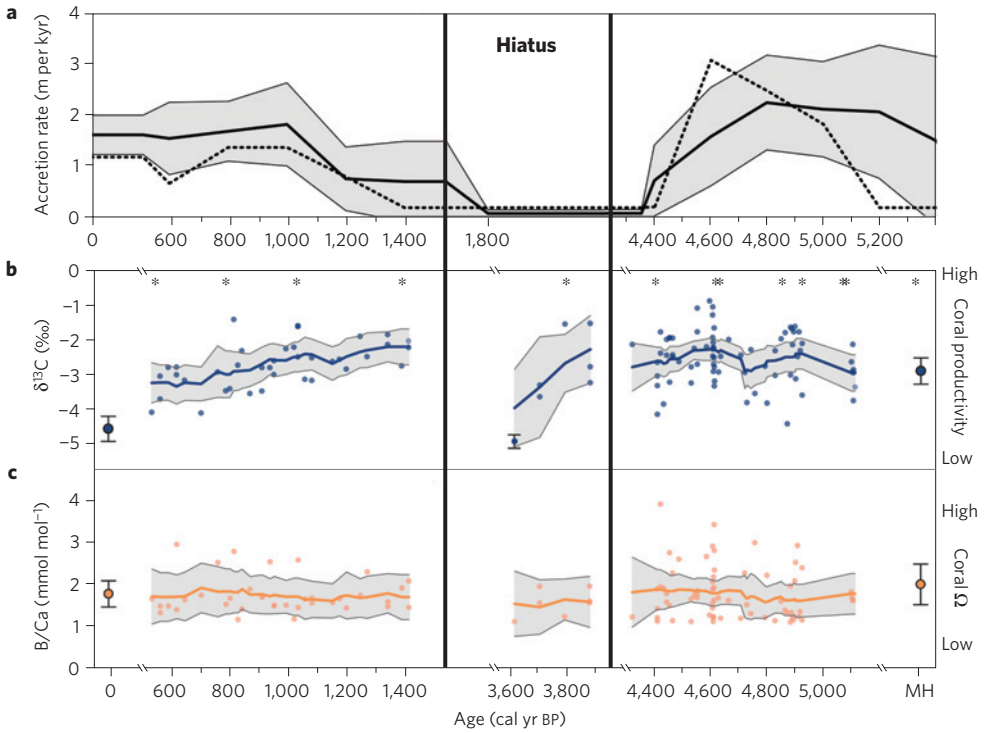

Figure 1 | Palaeoecological reconstructions of reef development in the Gulf of Panamá from the mid-Holocene (~6,750 cal yr BP) to present. Data are shown in relation to the hiatus in reef development (thick black outline). Bold lines represent 200-yr running means and grey shading represents the 95% CI. **a**, Reef accretion from the core used for geochemistry (dotted line) and variability from four additional cores from Contadora. **b**, Coral productivity (blue) from $\delta^{13}C$. The data from ~3,600 cal yr BP are shown as the mean ±95% CI of replicate samples. **c**, Internal aragonite saturation state of the corals (Ω; orange) from B/Ca. In **b**,**c**, measurements from mid-Holocene (MH) coral samples are aggregated into means (±95% CI), as are modern samples. Asterisks indicate the location of U-series dates used to construct an age model for the core.

coral holobiont[15,16]. Photosynthetic activity by the zooxanthellae preferentially fixes the lighter ^{12}C isotope, which enriches ^{13}C in the coral skeleton during periods of high coral productivity[15]. We thus interpret changes in $\delta^{13}C$ as an indicator of the productivity of the coral–zooxanthellae symbiosis[15,16]. Changes in B/Ca in foraminifera have been linked to carbonate saturation state at the internal sites of calcification, a relationship that is apparently independent of external pH (ref. 17). Variability in B/Ca is also independent of pH in corals[18], indicating that the mechanism by which boron is incorporated into coral skeletons may be similar. We interpret B/Ca in the coral skeletons as an indicator of the internal saturation state of the coral. We evaluated average trends in the geochemical data from multiple individuals within 200-yr time windows against observed changes in vertical reef accretion[8] (Supplementary Methods). Analysis of an ensemble of late-twentieth-century coral fragments allowed us to quantify within-population geochemical and isotopic variability, for comparison with potential signals in the palaeo-reconstructions.

Accretion was relatively slow when reef development initiated at Contadora ~6,750 cal yr BP (Fig. 1a). The geochemistry indicates that this period was cool, wet and characterized by moderate upwelling (Fig. 3), corroborating existing records of high oceanic productivity in the TEP from ~7,000–5,000 cal yr BP (refs 19,20). Our findings are consistent with a persistent, La Niña-like state in the tropical Pacific during the mid-Holocene[19–21].

Sea temperatures reconstructed from Sr/Ca reflect warming from ~19 °C at ~5,100 cal yr BP to ~25.5 °C at ~4,600 cal yr BP (Fig. 3a), which may be related to the decline in upwelling during that time (Fig. 3d,e). In contrast, $\delta^{18}O$ remained fairly stable over this period (Fig. 3b), suggesting that Pacific Panamá was relatively dry during the warmest interval (Fig. 3c). These changes are consistent with stronger or more frequent El Niño events, or a dampened seasonal cycle around 4,600 cal yr BP; however, this trend is not apparent in other records from the region[19,21]. Accretion rates were highest when temperature peaked ~4,600 cal yr BP, but declined precipitously in the run-up to the hiatus (Fig. 1a). Reconstructions of ΔR suggest that upwelling became significantly more intense and water temperatures cooled beginning 400 years before the hiatus (Fig. 3). Despite high environmental variability ~5,100–4,400 cal yr BP, average coral productivity and internal aragonite saturation state remained stable (Fig. 1b,c).

The physiological condition of the corals declined markedly at the onset of the hiatus. Coral productivity, as reflected by $\delta^{13}C$, was lower and more variable 3,900–3,600 cal yr BP than in any other part of our record (Fig. 1b). Indeed, six replicate analyses from the same coral confirm the anomalously low $\delta^{13}C$-value at ~3,600 cal yr BP. The fact that the other elemental ratios from this specimen—B/Ca, Sr/Ca, and Ba/Ca—fell within the range of other corals from the same period (Figs 2a,d and 1c) argues against a diagenetic explanation for the low ^{13}C-value. Average B/Ca was also 12% lower 3,900–3,600 cal yr BP than during the preceding centuries, although the trend was not significant. The decline in coral condition just before reef shutdown corroborates theoretical predictions that ecosystems on the brink of collapse exhibit early warning signs of increasingly wide ecological excursions and progressively slower rates of recovery from disturbance[9].

The observed environmental changes during the 300 yr following reef shutdown—significantly stronger upwelling, significantly cooler temperatures and higher precipitation (Fig. 3)—are consistent with a La Niña-like climate from 3,800 to 3,200 cal yr BP (ref. 21). We posit that more frequent or stronger La Niña events during this interval provided the initial physiological trigger that shut down reef accretion in Pacific Panamá. Elevated precipitation would have increased terrigenous input, resulting in higher turbidity

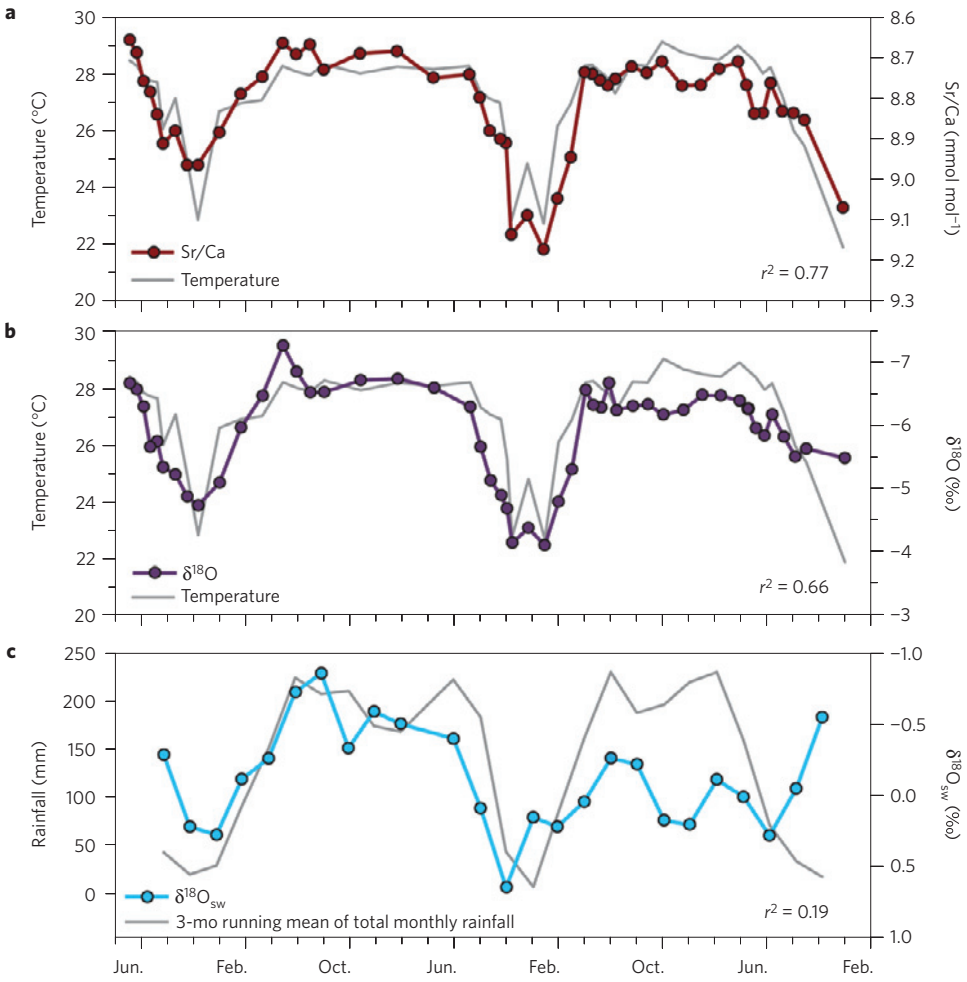

Figure 2 | Trends in Sr/Ca, $\delta^{18}O$ and $\delta^{18}O_{sw}$ in a representative modern colony of *Pocillopora damicornis* from Contadora Island, Gulf of Panamá, winter 2006–summer 2008. a, Relationship between Sr/Ca (red) and *in situ* temperature (grey). **b**, Relationship between $\delta^{18}O$ (purple) and *in situ* temperature (grey). **c**, Relationship between $\delta^{18}O_{sw}$ (cyan) and the three-month running mean of total monthly rainfall in Panamá City (grey).

and lower light penetration to the reef. Reduced water temperatures (Supplementary Fig. 1c) and decreased light penetration driven by more intense upwelling would have reduced coral productivity relative to heterotrophic feeding[15,16] and slowed *Pocillopora* growth rates[22]. Upwelling would have also decreased oceanic pH and aragonite saturation state[3], which could explain the 12% decline in B/Ca at the start of the hiatus. The onset of La Niña-like conditions triggered initial reef shutdown and enhanced ENSO variability continued to suppress reef development for the next two millennia[8].

As the hiatus also occurred in Panamá's Gulf of Chiriquí, where there is no upwelling[22], we infer that climatic cooling and a reduction in light initiated reef shutdown throughout the region. Increased upwelling would have further stressed the corals in the Gulf of Panamá, which explains the more protracted hiatus at Contadora relative to the Gulf of Chiriquí. Contemporaneous hiatuses in Costa Rica, Australia and Japan also occurred in low-light environments, consistent with our interpretation[8].

Reef accretion resumed at Contadora from 1,750 to 1,400 cal yr BP and remained high to present (Fig. 1a). Reduced ENSO variability and a more El Niño-like state[21,23] allowed Panamanian reefs to recover during the late Holocene. By 1,400 cal yr BP, the environment was characterized by relatively weak upwelling and a favourable regime of temperature and precipitation (Fig. 3). Upwelling intensity remained low in the Gulf of Panamá from 1,400 cal yr BP to present (Fig. 3d,e), but temperature and precipitation were more variable during the last millennium.

The Medieval Climate Anomaly (MCA; 1,150–700 cal yr BP) reflects relatively warm conditions that are similar, within error, to temperatures in the late twentieth century (Fig. 3a–c) and are consistent with an El Niño-dominated state in Pacific Panamá. In contrast, temperatures during the Little Ice Age (LIA; ~600–550 cal yr BP) were ~5 °C cooler (Fig. 3a–c), suggesting a return to La Niña-like conditions after the MCA. The LIA represents the coldest, wettest interval in our record. Reef accretion declined despite weak upwelling throughout the late Holocene, supporting our conclusion that changes in temperature and precipitation were the ultimate cause of the hiatus in Pacific Panamá. The suggestion that the MCA was characterized by a more El Niño-like state, whereas the LIA was more La Niña-like, is supported by reconstructions throughout the tropical Pacific[23,24]; however, there remains little consensus about the broad-scale impacts of the MCA and the LIA on the region[25,26].

A steady decrease in coral $\delta^{13}C$ from 1,400 cal yr BP to present suggests that coral productivity declined in the recent past. The anomalously low $\delta^{13}C$ of modern corals (Fig. 1b) is primarily a result of the so-called ^{13}C Suess effect: a decrease in atmospheric $\delta^{13}C$ caused by the burning of fossil fuels[27]. Cooler sea temperatures during the LIA may explain the low coral productivity after 600 cal yr BP, but temperatures were higher from 1,400 to 600 cal yr BP (Fig. 3). Another possible cause of declining coral productivity is the putative increase in the frequency of El Niño events in recent millennia[21,23]. El Niño events cause high-temperature

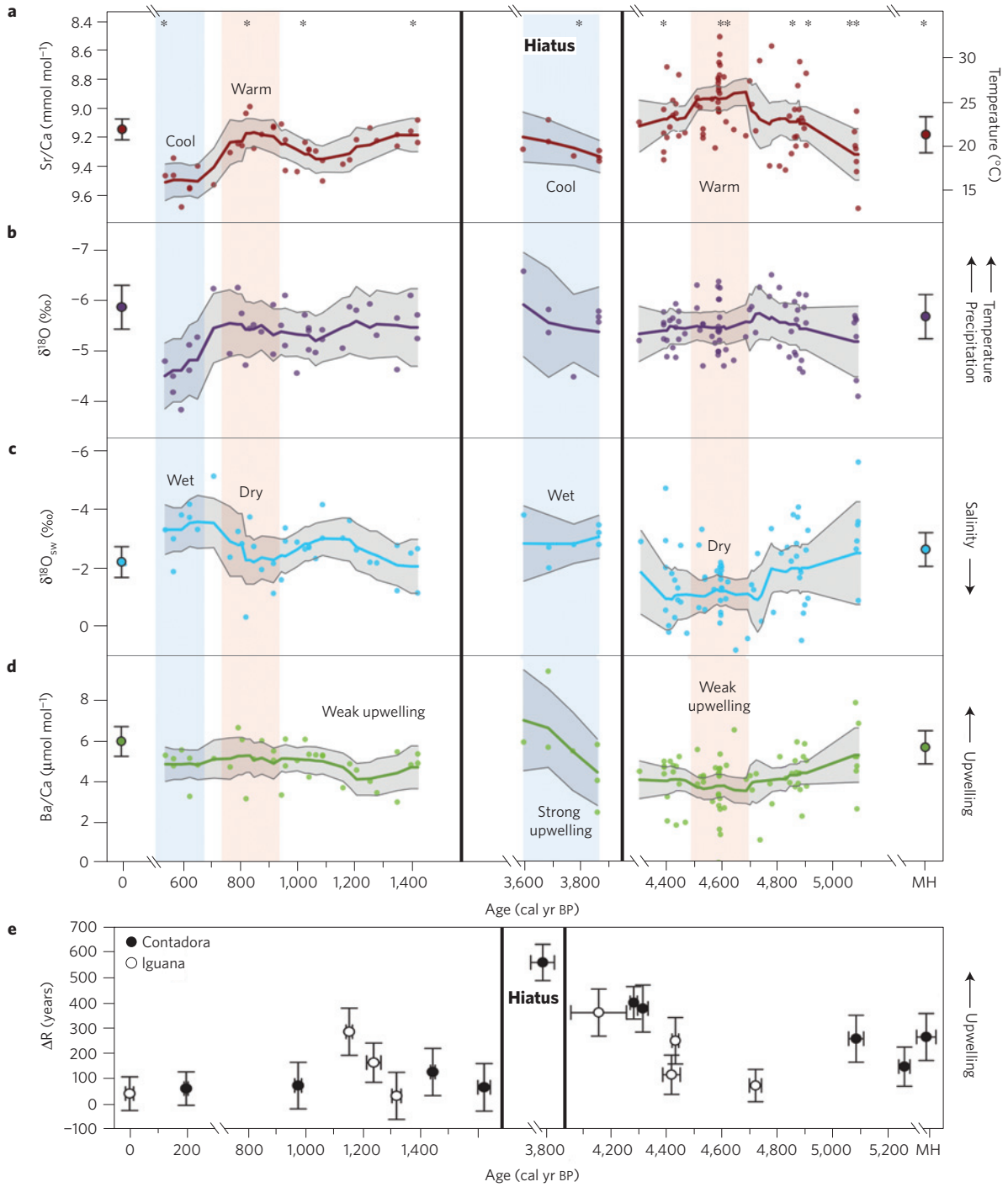

Figure 3 | Environmental variability in the Gulf of Panamá from the mid-Holocene (~6,500 cal yr BP) to present. Data are shown in relation to the hiatus in reef development (thick black outline). Bold lines represent 200-yr running means and grey shading represents 95% CIs. **a**–**c**, Palaeoclimatic reconstructions were derived from: Sr/Ca-based temperature reconstructions (red; **a**), combined temperature and precipitation from $\delta^{18}O$ (purple; **b**) and $\delta^{18}O_{sw}$ (salinity) calculated by subtracting the reconstructed Sr/Ca-based temperatures from the $\delta^{18}O$ signature of the corals (cyan; **c**). **d**,**e**, Reconstructions of upwelling from: Ba/Ca (green; **d**), and ΔR from Contadora (black) and Iguana Islands (white; **e**). In **b**,**c**, measurements from the mid-Holocene (MH) coral samples are aggregated into means (±95% CI), as are the modern samples. Asterisks indicate the location of U-series dates used to construct an age-model for the core.

stress and coral bleaching, reducing coral productivity and driving $\delta^{13}C$ to more negative values[16].

Despite high environmental variability and declining coral productivity during the late Holocene, B/Ca varied little from 1,400 to 550 cal yr BP (Fig. 1c). The precision of our B/Ca measurements was low relative to the range of measured B/Ca (Supplementary Table 3), which may partially explain this result. Upwelling reduces the pH of sea water, which leads to lower carbonate saturation states in upwelling regions[3]. Assuming that B/Ca reflects corals' internal saturation state[17,18], B/Ca should be strongly and negatively correlated with indicators of upwelling such as ΔR and Ba/Ca if internal saturation state is purely a function of the external environment. The only detectable, albeit nonsignificant decline in B/Ca—12%—occurred during the onset of the hiatus, when

upwelling intensity was higher, and pH presumably lower, than at any other time in the record.

Secular trends in ocean acidification through the Holocene[28] suggest that changes in carbonate chemistry did not drive the observed hiatus. Our results are consistent with the suggestion that corals have the capacity to buffer their internal carbonate chemistry against changes in the external environment and, therefore, might not be noticeably affected by the changes in oceanic acidity expected in the near future[2,29]. The projected increase in extreme thermal stress over the coming decades will cause enormous damage to coral reefs before the impacts of ocean acidification on corals are realized[1,29].

Although these results are derived from a single core, the high degree of replication inherent in our sampling strategy allows us to calculate a robust estimate of the uncertainties in our coral reconstructions. Our geochemical and isotopic data from core EP09-28 suggest that the reef at Contadora was remarkably resistant to climatic and oceanographic variability over the past 6,750 years. Reef development persisted despite marked variations in upwelling intensity, precipitation and average sea temperatures that ranged from 16 to 26 °C (from Sr/Ca) outside the hiatus. At the onset of the hiatus, however, the reef reached a critical ecological and environmental threshold beyond which coral growth and vertical framework accretion could not be sustained. The reef was growing in at least 1.5 m of water (relative to mean sea level) since initiation (Supplementary Fig. 2), excluding sea level as the primary cause of significant palaeoecological change. Environmental shifts after ~4,100 cal yr BP were associated with marked changes in the palaeophysiology of the corals, most notably the decline in coral productivity ($\delta^{13}C$). The inferred environmental tipping point was followed by a decline in coral growth and then whole-reef degradation[8,9].

Climatic and oceanographic variability controlled the growth of coral populations and the development of coral reefs in the tropical eastern Pacific during the Holocene. If the sublethal trend of declining coral productivity at the onset of the hiatus was an early warning sign of deteriorating ecosystem state and impending collapse[9], then the decline of coral productivity during the late Holocene could likewise portend a reef shutdown. Whereas the 2,500-yr collapse of Panamanian reefs was provoked by a shift to a cooler climate, anthropogenic climate change is now increasing sea temperatures on a global scale. Average sea temperatures at Contadora are now within only a few degrees of the maximum temperatures that supported coral growth during the Holocene (Fig. 3a). In a global coral-reef landscape characterized by declining coral cover, reduced growth and calcification, and negative trajectories of reef accretion, mitigating and reversing anthropogenic climate change are critical steps to ensuring the continuity of coral populations, reef-framework accretion, and the ecosystem services that coral reefs provide[1–7].

Methods

We developed temperature calibrations for *Pocillopora damicornis* by relating the Sr/Ca and $\delta^{18}O$ profiles of three modern corals from Contadora to *in situ* temperatures measured for the period during which the corals grew. We drilled the skeletons of the corals at submonthly resolution along their longitudinal growth axes. The resulting 72 samples were analysed for Sr/Ca and $\delta^{18}O$ in K.M.C.'s laboratory. $\delta^{18}O$ was measured on ThermoFisher Delta Plus V with a Kiel device. Average reproducibility of standards (1σ) was less than ±0.06‰ on average. Sr/Ca was measured on a HORIBA Jobin-Yvon Ultima 2C inductively coupled plasma-optical emission spectrometer. Average reproducibility of standards (1σ) was less than ±0.07%.

For the palaeoenvironmental reconstructions, we extracted a 268-cm core of *Pocillopora*-dominated reef framework from Contadora Island (8° 37′ 60″ N, 79° 01′ 44″ W), in the Gulf of Panamá upwelling system. Coral skeletons were dated throughout the core ($n=17$; asterisks in Figs 1 and 3) using U/Th analysis by inductively coupled plasma mass spectrometry (Supplementary Table 4). The U-series dates were used to create an age model for the geochemical data (Supplementary Fig. 7).

A total of 133 subfossil *Pocillopora* branch fragments in good taphonomic condition were sampled in a roughly even distribution throughout the core for geochemical analysis. Scanning electron microscopy showed diagenetic alteration to be negligible (Supplementary Fig. 4). The branch fragments were split longitudinally and drilled along their growth axes using a micromill. Carbonate powders from each branch fragment were combined into a homogenized sample representing ~1–2 yr of coral growth[22].

Geochemical analyses of the subfossil branch fragments were conducted at the Stable Isotope Laboratory at the Rosenstiel School of Marine and Atmospheric Science. Stable-isotope ratios ($\delta^{18}O$ and $\delta^{13}C$) were measured using standard techniques on a Thermo-Finnigan Delta Plus mass spectrometer with a Kiel device. Reproducibilities (1σ) of the in-house standard—optically clear calcite—were less than ±0.10 ‰ for $\delta^{18}O$ and $\delta^{13}C$. Elemental concentrations of strontium (Sr), barium (Ba) and boron (B) were measured with a Varian Vista-PRO CCD (charge-coupled device) simultaneous inductively coupled plasma-optical emission spectrometer using standard techniques. Analytical precisions (1σ) of measurement on the in-house element-to-calcium standard were ±0.02% for Sr/Ca, ±0.19% for Ba/Ca, and ±0.55% for B/Ca.

We used our modern temperature calibration for Sr/Ca and $\delta^{18}O$ in *Pocillopora* to derive palaeotemperatures from the core record. Relative palaeosalinities ($\delta^{18}O_{sw}$) were then calculated by subtracting each Sr/Ca temperature signal from the corresponding $\delta^{18}O$ value. All other geochemical tracers were evaluated on a relative scale. Geochemical data are presented as 200-yr running means with 95% confidence intervals (CIs). Each 95% CI is a combined error that incorporates the uncertainty associated with analytical precision, geochemical variability within individual corals (Supplementary Table 1), variability among corals growing contemporaneously in the same environment (Supplementary Table 2), and variability among corals within the 200-yr window. The procedure for quantifying these uncertainties is described in the Supplementary Methods.

The local reservoir correction, ΔR, provides a measure of the offset between the conventional radiocarbon ages and the true ages of samples collected in the marine environment[8]. Upwelling reintroduces old carbon from deep waters to the surface, which increases the apparent age of shallow water-masses in upwelling regions. Thus, ΔR is a proxy for changes in upwelling intensity. We collected individual fragments of *Pocillopora* ($n=15$) and *Psammocora stellata* ($n=3$) from 5 cores from Contadora Island ($n=12$) and 4 cores from Iguana Island ($n=7$), both of which are located in the upwelling-influenced Gulf of Panamá[8]. Each coral fragment, weighing 0.5–3 mg, was broken into two samples for dating. One sample from each coral was ^{14}C-dated using accelerator mass spectrometry at the National Ocean Sciences AMS (NOSAMS) facility at Woods Hole and the other was dated by U/Th using inductively coupled plasma mass spectrometry by H.C. and R.L.E. Treating U/Th age as the true age, we obtained the expected radiocarbon age of that sample from the global marine calibration curve. The difference between the measured and expected radiocarbon ages of the coral yielded ΔR (Supplementary Methods).

The palaeoenvironmental data were evaluated against vertical reef accretion rates for Contadora and the proxies for palaeophysiology of the corals: $\delta^{13}C$ and B/Ca. We calculated millennial-scale rates of reef accretion (in m per kyr) from core EP09-28 and four additional cores from Contadora. The five cores were dated using a combination of bulk ^{14}C-dating with standard techniques (Beta Analytic), ^{14}C-dating by accelerator mass spectrometry (NOSAMS), and U-series dating (H.C. and R.L.E.). Vertical-accretion rates were calculated by dividing the length of an interval in the core, corrected for compaction, by the time over which that interval was deposited.

Received 30 June 2014; accepted 16 January 2015; published online 23 February 2015

References

1. Donner, S. D. Coping with commitment: Projected thermal stress on coral reefs under different future scenarios. *PLoS ONE* **4,** e5712 (2009).
2. Pandolfi, J. M., Connolly, S. R., Marshalland, D. J. & Cohen, A. L. Projecting coral reef futures under global warming and ocean acidification. *Science* **333,** 418–422 (2011).
3. Manzello, D. P. *et al.* Poorly cemented coral reefs of the eastern tropical Pacific: Possible insights into reef development in a high-CO_2 world. *Proc. Natl Acad. Sci. USA* **105,** 10450–10455 (2008).
4. De'ath, G., Lough, J. M. & Fabricius, K. E. Declining coral calcificaton on the Great Barrier Reef. *Science* **323,** 116–119 (2009).
5. Cantin, N. E., Cohen, A. L., Karnauskas, K. B., Tarrant, A. M. & McCorkle, D. C. Ocean warming slows coral growth in the central Red Sea. *Science* **329,** 322–325 (2010).
6. Perry, C. T. *et al.* Caribbean-wide decline in carbonate production threatens coral reef growth. *Nature Commun.* **4,** 1402 (2013).
7. Alvarez-Filip, L., Carricart-Ganivet, J. P., Horta-Puga, G. & Iglesias-Prieto, R. Shifts in coral-assemblage composition do not ensure persistence of reef functionality. *Sci. Rep.* **2,** srep03486 (2013).
8. Toth, L. T. *et al.* ENSO drove 2500-year collapse of eastern Pacific coral reefs. *Science* **337,** 81–84 (2012).

9. Scheffer, M. *et al.* Early-warning signals for critical transitions. *Nature* **461,** 53–59 (2009).
10. Kiessling, W. Geologic and biologic controls on the evolution of reefs. *Ann. Rev. Ecol. Evol. Syst.* **40,** 173–192 (2009).
11. Dixit, Y., Hodell, D. A. & Petrie, C. A. Abrupt weakening of the summer monsoon in northwest India ~4100 yr ago. *Geology* **42,** 339–342 (2014).
12. Liu, Z. *et al.* Paired oxygen isotope records reveal modern North American atmospheric dynamics during the Holocene. *Nature Commun.* **5,** 3701 (2014).
13. Nurhati, I. S., Cobb, K. M. & DiLorenzo, E. Decadal-scale SST and salinity variations in the central Tropical Pacific: Signatures of natural and anthropogenic climate change. *J. Clim.* **24,** 3294–3308 (2011).
14. Shen, G. T. *et al.* Surface ocean variability at Galapagos from 1936–1982: Calibration of geochemical tracers in corals. *Paleoceanography* **7,** 563–588 (1992).
15. Grottoli, A. G. & Wellington, G. M. Effect of light and zooplankton on skeletal δ^{13}C values in the eastern Pacific corals *Pavona clavus* and *Pavona gigantea*. *Coral Reefs* **18,** 29–41 (1999).
16. Suzuki, A. *et al.* Skeletal isotope microprofiles of growth perturbations in *Porites* corals during the 1997–1998 mass bleaching event. *Coral Reefs* **22,** 357–369 (2003).
17. Yu, J. & Elderfield., H. Benthic foraminiferal B/Ca ratios reflect deep water carbonate saturation state. *Earth Planet. Sci. Lett.* **258,** 73–86 (2007).
18. Allison, N., Finch, A. A. & EIMF, δ^{11}B, Sr, Mg and B in a modern *Porites* coral: The relationship between calcification site pH and skeletal chemistry. *Geochim. Cosmochim. Acta* **74,** 1790–1800 (2010).
19. Koutavas, A. & Joanides, S. El Niño–Southern Oscillation extrema in the Holocene and Last Glacial Maximum. *Paleoceanography* **27,** PA4208 (2012).
20. Pennington, J. T. *et al.* Primary production in the eastern tropical Pacific: A review. *Prog. Oceanogr.* **69,** 285–317 (2006).
21. Conroy, J. L., Overpeck, J. T., Cole, J. E., Shanahan, T. M. & Steinitz-Kannan, M. Holocene changes in eastern tropical Pacific climate inferred from a Galápagos lake sediment record. *Quat. Sci. Rev.* **27,** 1166–1180 (2008).
22. Glynn, P. W. Coral growth in upwelling and nonupwelling areas off the Pacific coast of Panama. *J. Mar. Res.* **35,** 567–585 (1977).
23. Yan, H. *et al.* A record of the Southern Oscillation Index for the past 2,000 years from precipitation proxies. *Nature Geosci.* **4,** 611–614 (2011).
24. Oppo, D. W., Rosenthal, Y. & Linsley, B. K. 2000-year-long temperature and hydrology reconstructions from the Indo-Pacific warm pool. *Nature* **460,** 1113–1116 (2009).
25. Cobb, K. M., Charles, C. D., Cheng, H. & Edwards, R. L. El Niño/Southern Oscillation and tropical Pacific climate during the last millennium. *Nature* **424,** 271–276 (2003).
26. Rein, B., Lückge, A. & Sirocko, F. A major Holocene ENSO anomaly during the Medieval period. *Geophys. Res. Lett.* **31,** L17211 (2004).
27. Swart, P. K. *et al.* The ^{13}C Suess effect in scleractinian corals mirror changes in the anthropogenic CO_2 inventory of the surface oceans. *Geophys. Res. Lett.* **37,** L05604 (2010).
28. Riding, R., Liang, L. & Braga, J. C. Millennial-scale ocean acidification and late Quaternary decline of cryptic bacterial crusts in tropical reefs. *Geobiol.* **12,** 387–405 (2014).
29. McCulloch, M., Falter, J., Trotter, J. & Montagna, P. Coral resilience to ocean acidification and global warming through pH up-regulation. *Nature Clim. Change* **2,** 623–627 (2012).

Acknowledgements

We are grateful to P. Swart, A. Rosenberg and A. Waite for providing assistance with geochemical analyses. We also thank M. Bush, P. Glynn, J. Trefry and R. van Woesik for advice and discussion. H. Guzmán and S. Dos Santos of the Smithsonian Tropical Research Institute provided regional temperature and rainfall data for the proxy calibrations. This research was financially supported by a Graduate Student Research Grant from the Geological Society of America, a grant from the Lerner–Gray Fund for Marine Research of the American Museum of Natural History, grants from the Smithsonian Institution's Marine Science Network, and the Natural Science Foundation of China grant no. 41230524. Field work was carried out under permits from the Republic of Panamá. This paper is dedicated to the memory of G. M. Wellington, whose research in the eastern Pacific laid the foundations on which our work is built. This is Contribution 128 from the Institute for Research on Global Climate Change at the Florida Institute of Technology.

Author contributions

L.T.T. conceived and designed the study, analysed the data, and wrote the paper. R.B.A. designed the study and wrote the paper. K.M.C. analysed the data and wrote the paper. H.C. and R.L.E. analysed the U-series data. P.R.G. and H.R.S. analysed the modern geochemical samples. All authors contributed to the discussion of results.

Additional information

The geochemical data set is available online in NOAA's Paleoclimatology database (http://www.ncdc.noaa.gov/paleo/study/17915). Supplementary information is available in the online version of the paper. Reprints and permissions information is available online at www.nature.com/reprints. Correspondence and requests for materials should be addressed to L.T.T.

Competing financial interests

The authors declare no competing financial interests.

nature climate change

SUPPLEMENTARY INFORMATION

DOI: 10.1038/NCLIMATE2541

Climatic and biotic thresholds of coral-reef shutdown

Lauren T. Toth[1], Richard B. Aronson[1,2], Kim M. Cobb[3], Hai Cheng[4,5], R. Lawrence Edwards[5], Pamela R. Grothe[3], Hussein R. Sayani[3]

[1] Department of Biological Sciences, Florida Institute of Technology, Melbourne, FL 32901, USA.
[2]Smithsonian Marine Station and National Museum of Natural History, Smithsonian Institution, Washington, DC 20560, USA.
[3]Department of Earth and Atmospheric Sciences, Georgia Institute of Technology, Atlanta, GA 30332, USA.
[4] Institute of Global Environmental Change, Xi'an Jiaotong University, Xi'an 710049, China.
[5] Department of Earth Sciences, University of Minnesota, Minneapolis, MN 55455, USA.

Supplementary Discussion

Upwelling

Upwelling is the most important source of intra-annual variability in Pacific Panamá. In the Gulf of Panamá, seasonal upwelling is driven by the annual migration of the Inter-Tropical Convergence Zone (ITCZ) between 10° and 3° N (ref. 30). Each year during the boreal winter (December through mid-April), the ITCZ migrates south of the Isthmus of Panamá, leading to intensification of the northeast trade winds across the region[30–32]. The Gulf of Panamá is adjacent to a topographic low in the Central American cordillera, which allows the trade winds to cross the Isthmus. These winds force surface waters offshore and bring cold, nutrient-rich, deep water from offshore onto the shelf[32] (Supplementary Fig. 1a). Because of the topographic differential along the Panamanian Isthmus, there is a pronounced gradient in upwelling strength along Panamá's Pacific coast. Upwelling is most intense in around the Pearl Islands archipelago, where Contadora is located[8] (Fig 1a).

The cold sea temperatures and high levels of some nutrients associated with upwelling in the Gulf of Panamá result in slower growth rates of the dominant framework-building coral,

Pocillopora damicornis, relative to the non-upwelling Gulf of Chiriquí[22] (but see ref.33). Likewise, coral growth in the Gulf of Panamá is depressed during the upwelling season compared with the rest of the year[34]. Additionally, because oceanic deep-water typically has a lower pH than surface waters, seasonal upwelling depresses the regional carbonate saturation state throughout the TEP, but especially in upwelling centers like the Gulf of Panamá[3].

El Niño–Southern Oscillation

El Niño–Southern Oscillation (ENSO) is a major source of interannual climate variability around the world, but its impacts are particularly important across the tropical Pacific Ocean[30]. In the TEP, both the El Niño and La Niña phases of the oscillation have major environmental impacts. El Niño results in a warming of sea temperatures throughout the TEP[35] (Supplementary Fig. 1b). In Pacific Panamá, El Niño events are also associated with low cloud cover and decreased precipitation because the Central American monsoon is suppressed and the dry season is more protracted[36–38]. As a result of high sea temperatures and high insolation, Panamanian reefs can experience severe coral bleaching during El Niño years[39].

During La Niña events, water temperatures are cooler than average in the TEP as a result of shoaling of the thermocline (Supplementary Fig. 1c) and sea level is reduced relative to the western Pacific[40]. Reefs in the TEP experience more frequent subaerial exposure during La Niña than at other times, which can result in high levels of coral mortality[41,42]. Additionally, enhanced rainfall during La Niña events in some parts of the TEP, including Pacific Panamá[36–38], can lead to highly turbid conditions because of enhanced coastal runoff[41], potentially resulting in limited light availability and reduced coral growth[43]. Finally, La Niña is associated with a strengthening of the northeast trade winds, which increases upwelling in some parts of the TEP[30,44].

Holocene sea-level change

There is significant uncertainty about the Holocene sea-level history of the TEP; however, it is generally assumed that the sea-level curve for this region resembles that of the Caribbean, where the last 6000 years were characterized by a gradual rise in sea level to present. Core EP09-28 was taken in 4 m of water (relative to mean sea level, or MSL). We plotted the depths of dated samples in our cores against the Toscano–Macintyre sea-level curve for the Caribbean[45] (Supplementary Fig. 2). Our plot shows that, although the reef was likely exposed periodically during low-tide events, the reef grew at a depth of at least 1.5 m (MSL) throughout its Holocene history. A sea-level highstand during the mid-Holocene, which has been described for some parts of the western Pacific[46,47], would have implied a more rapid rise in sea level than in the Caribbean after reef initiation and an even higher sea level at the start of the hiatus. We suggest, therefore, that although sea level undoubtedly had some impact on Holocene reef development in Pacific Panamá it was not the primary cause of the hiatus.

Supplementary Methods

Collection and description of the core

The 2.68-m core used in this study, core EP09-08, was collected from unconsolidated *Pocillopora* reef framework of the fore-reef slope of Contadora Island in the Pearl Islands using the push-coring methodology described previously[8]. In the laboratory, the core was frozen and then split longitudinally using a band saw with a diamond-tipped blade. The core was thawed and one half was used for geochemical analysis. The other half was divided into 5-cm sections and sieved to separate carbonate material >2 mm in longest dimension from the sedimentary matrix. Material >2 mm was cleaned with high-pressure water and sorted by species and taphonomic condition. The masses of the constituents within each 5-cm interval were used to identify distinct layers within the core representing periods of active or interrupted reef growth. Detailed methodologies of the paleoecological analysis can be found in ref. 8. Core EP09-28 was composed primarily of skeletons of the branching coral *Pocillopora* spp. in good taphonomic condition (<25% surface alteration; Supplementary Fig. 3); however, skeletons of the free-living coral *Psammocora stellata* and branching coralline algae were abundant within the more degraded material delimiting the hiatus (~4100–1600 cal BP).

Sampling of coral skeletons for Holocene reconstructions

In the half of core EP09-28 used for geochemical analyses, all *Pocillopora* spp. corals were collected and their exact depths within the core were recorded. A total of 133 *Pocillopora* corals in good-to-excellent taphonomic condition (<20% surface alteration) were sampled approximately evenly throughout the core for geochemical analysis. Sampling effort was increased for the 500-yr period just before the hiatus, in case high-resolution sampling during this interval could provide insights into the conditions leading to reef collapse. In order to avoid

surface contamination, we sampled the pristine internal skeletons of the corals by splitting them longitudinally using a Pelco PCS-400 diamond-blade saw dedicated to that purpose. Carbonate powders were collected from the internal skeletons using a Sherline 5100 micromill dedicated to carbonate sampling. Corals were drilled in several locations along their growth axes and the powders were combined to create a single, homogenized sample for that coral. Such samples represented average conditions over ~1–2 years of growth, assuming *Pocillopora* in Pacific Panamá grows ~3 cm per year[22] (Fig. 2).

Diagenetic screening

Although only the most pristine samples were selected for geochemical analysis, there remained the possibility of minor post-depositional alteration of the coral skeletons. Diagenetic alteration is especially problematic for trace-element analysis, but it can lead to significant errors in stable-isotope measurements as well[48]. Using scanning electron microscopy (SEM), we visually evaluated a random subsample of 20 corals to evaluate the potential for diagenesis. The samples were gold-coated with a Denton Vacuum Desk III and imaged using the JEOL JSM-6380LV SEM in the Department of Biological Sciences at the Florida Institute of Technology.

We found virtually no evidence of diagenetic alteration in the 20 coral samples evaluated with SEM. All the corals appeared to be composed of primary aragonite (Supplementary Fig. 4a–t); however, one degraded section of one coral from an unsampled section of one of the corals did contain some crystals of secondary aragonite (Supplementary Fig. 4u), and another coral contained a small section with carbonate cements (Supplementary Fig. 4v). Importantly, none of the sampled sections of the corals appeared to contain any secondary carbonate precipitation. Additional SEM images of these corals can be found in ref. 49.

Quantifying uncertainty

To calculate the uncertainties inherent in our estimates of mean environmental conditions during the middle to late Holocene, we calculated a combined error estimate from the following error sources, measured as standard deviations:

1. analytical uncertainty (instrumental precision);
2. variability within corals (as a result of incomplete homogenization of samples);
3. variability among corals growing over the same time-period; and
4. variability across a 200-year time-window.

The analytical precisions of elemental and isotopic measurements (error 1) were derived from replicate analysis of the in-house standard in P. Swart's lab, which is optically clear calcite (OCC), during the course of the analysis. Standard deviation of OCC replicates was less than ±0.10‰ for $\delta^{18}O$ and $\delta^{13}C$. The residual standard deviations of the element-to-calcium ratios for the in-house standards were 0.02% for Sr/Ca, 0.19% for Ba/Ca, and 0.55% for B/Ca.

Samples collected along the growth axes of our Holocene corals were combined and mixed to create a bulk sample for each coral; however, it is possible that these samples were not completely homogenized. To account for this potential source of error (error 2), we measured the variability in replicate subsamples from bulk-sampled modern corals collected alive at Contadora in 2008 and 2009. For $\delta^{18}O$ and $\delta^{13}C$, we were able to obtain five replicate samples from each of four modern corals. For the element-to-calcium ratios, the small amount of remaining coral powder from the corals limited our sampling to four replicates from one coral and three replicates from a second coral. The standard deviations of geochemical ratios for each of the replicate subsamples are given in Supplementary Table 1. We used the average standard deviation of the four corals as an estimate of within-coral variability.

Genetic variability and/or microhabitat differences among individual corals samples is another potential source of variability. We assessed among-colony variability (error 3) by measuring the bulk geochemistry over ~1 year (upper ~35 mm) of 11 corals collected alive at Contadora in 2008 and 10 corals collected in 2009. Four corals (CL-4 and CL-15 from 2008, and CL-12 and CL-21 from 2009) were subsampled for the analysis of within-coral variability described above. The results of these analyses are given in Supplementary Table 2.

We calculated 200-year running means of each geochemical variable during the Holocene. The final source of error we considered was the standard deviation of coral geochemistry within the 200-yr windows (error 4). The standard deviation combining these sources of error was calculated as the root-sum-square of the standard deviations quantifying the individual sources of error using the following equation:

$$SD_{total} = \sqrt{{SD_{(1)}}^2 + {SD_{(2)}}^2 + {SD_{(3)}}^2 + {SD_{(4)}}^2} \qquad [1]$$

We applied the average values for $SD_{(2)}$ and $SD_{(3)}$ calculated from modern corals across the Holocene record. $SD_{(1)}$ was also held constant. In contrast, $SD_{(4)}$ varied through time based on the number of samples and the environmental variability of the ecosystem within each 200-yr window. We used the combined errors to calculate 95% confidence intervals (95% CI) for the 200-yr running means (Figs. 1 and 3) according to the following equation:

$$95\%\ CI = \left({SD_{total}} \Big/ \sqrt{n_{200}} \right) \times 1.96 \qquad [2]$$

where n_{200} is the number of samples falling within a 200-yr window at any given point. Because the 95% CI of the mean geochemical values are robust and comprehensive, we can use these error terms to evaluate changes in coral geochemistry statistically during the past ~6750 years.

After quantifying the total uncertainty in our geochemical data, we evaluated the sensitivity of the Holocene dataset by comparing the measured range of each proxy to the average error associated with the proxy (average 95% CI). These data are summarized in Supplementary Table 3. The ranges of both the raw geochemical data and the 200-yr running means of those data are generally larger than the error terms, validating our statistical ability to detect long-term changes in the environment and the physiology of the corals using the geochemical proxies. Indeed, for all the proxies except B/Ca, variability through time in the Holocene is more than twice the error. Although the overall range of B/Ca is higher than the error term, the range of the running mean is narrower, suggesting that long-term variability in B/Ca may be at the limit of detectability using our methodologies. We interpret B/Ca with caution.

Temperature calibrations derived for *Pocillopora*

To date, only one Sr/Ca and two $\delta^{18}O$ temperature calibrations have been derived for *Pocillopora damicornis*[50–52], and they have not been updated since the early 1980s. We derived temperature calibrations for *P. damicornis* by relating the Sr/Ca and $\delta^{18}O$ profiles of three modern corals from Contadora to *in situ* temperatures measured for the period during which the corals grew. Coral fragments CL-1 and CL-2, which were both 45 mm long, were collected alive in the Summer of 2011 and had been growing since the winter of 2010 (Supplementary Fig. 5) adjacent to a HOBO Pendant® temperature logger we had deployed on Contadora reef during

the summer of 2009. *In situ* temperature data from Contadora were not available for a 150 mm long coral, CL-4, which was collected in the summer of 2009. For this coral, we used temperature data from the long-term monitoring station at nearby Pedro-Pablo Island (~30 km from Contadora and also in the Pearl Islands archipelago), which is maintained by H. Guzman and S. Dos Santos of the Smithsonian Tropical Research Institute. Concurrent temperature measurements at Contadora and Pedro-Pablo from 2009–2010 suggest that annual temperature variability is similar at the two sites (Pearson correlation: r=0.95, P<0.001). Average temperature was 28.4±1.2 (SD) at Contadora and 28.1 ±1.2 at Pedro-Pablo over this period.

Corals CL-2 and CL-4 were drilled every 2 mm along their longitudinal growth axes (~20 samples per year) for Sr/Ca and $\delta^{18}O$ analysis. Coral CL-1 was drilled every 1 mm (~35 samples per year). Both sampling regimes provided a submonthly geochemical profile of the corals for a total of 72 samples. The corals were analyzed for Sr/Ca and $\delta^{18}O$ in K.M.C.'s laboratory at the Georgia Institute of Technology. $\delta^{18}O$ was measured on ThermoFisher Delta Plus V with a Kiel device. Average error in the reproducibility of standards (1σ) was less than ±0.06‰. Sr/Ca was measured on a HORIBA Jobin-Yvon Ultima 2C Inductively Coupled Plasma-Optical Emission Spectrometer. Average reproducibility of standards (1σ) was less than 0.07% on average.

We identified 25 unique tiepoints during the periods over which our *in situ* temperature and coral-geochemistry records overlapped, and we used them to develop age-models for the corals by linear interpolation using the zoo package in R Studio[53–55]. We then calculated weekly running means of the daily average *in situ* temperatures for each interpolated date. Least-squares linear regression was used to compare coral-based measurements of temperature to Sr/Ca and $\delta^{18}O$ using R Studio.

We derived the following relationship between temperature and Sr/Ca in *P. damicornis* at Contadora, for which r^2=0.77 (Fig. 2b; Supplementary Fig. 6; $F_{1, 71}$=238.9, P<0.001):

$$Sr/Ca_{coral}=10.493–0.0612(T°C) \quad [3]$$

The relationship between temperature and $\delta^{18}O$ in the corals was:

$$\delta^{18}O_{coral}=5.514–0.417(T°C) \quad [4]$$

for which r^2=0.66 (Fig. 2c; Supplementary Fig. 6; $F_{1,70}$=140.1, P<0.001). As expected, the relationship between temperature and $\delta^{18}O$ was not as strong as that between temperature and Sr/Ca. Whereas Sr/Ca in coral skeletons is primarily driven by temperature, the $\delta^{18}O$ signature is also strongly driven by changes in salinity ($\delta^{18}O_{sw}$; ref. 13).

We used the calibration for Sr/Ca to derive paleotemperatures from the core records, and $\delta^{18}O$ was reported on a relative scale. Relative paleosalinities ($\delta^{18}O_{sw}$) were then calculated by subtracting each Sr/Ca temperature estimate from the corresponding $\delta^{18}O$-derived value. We compared monthly averages of $\delta^{18}O_{sw}$ from the modern coral CL-4 to seasonal (three-month) running means of total monthly rainfall from the closest weather station to Contadora, the Balboa Heights station in Panamá City (08°57'34"N, 79°33'15"W; ~68 km from Contadora). Although the relationship between the rainfall and $\delta^{18}O_{sw}$ was not particularly strong (r^2=0.19), it was significant ($F_{1,24}$=5.514, P=0.028) and the seasonal pattern of rainfall is reflected in the $\delta^{18}O_{sw}$ trends. Furthermore, rainfall is highly variable over small spatial scales in Panamá, and we would expect local rainfall at Contadora to be more strongly correlated with coral $\delta^{18}O_{sw}$ there. We conclude, therefore, that precipitation is the primary driver of $\delta^{18}O_{sw}$ variability at this site, corroborating previous results[51].

Local reservoir correction

The local reservoir correction, ΔR (analogous to $\Delta^{14}C$), provides a measure of the offset between the radiocarbon ages and the true ages of samples collected in the marine environment[56,57]. Upwelling reintroduces old carbon from deep waters to the surface, which increases the apparent age of shallow-water masses in upwelling regions. The difference between radiocarbon ages, which are biased toward older dates, and the more accurate U/Th ages[58] can be used to calculate ΔR (ref. 56). We quantified temporal variations ΔR from coral skeletons in the Gulf of Panamá as a proxy of changes in upwelling intensity from ~6750 cal BP to present[59–60].

We collected individual fragments of *Pocillopora* (n=15) and *Psammocora stellata* (n=3) from 5 cores from Contadora Island (n=12) and 4 cores from Iguana Island (n=7). Both sites are located in the upwelling-influenced Gulf of Panamá. Using previously established age-models for the cores[8], we chose samples to provide the highest possible temporal resolution between ~6750 cal BP and present. Each coral fragment, weighing 0.5–3 mg, was broken into two samples for dating. One sample from each coral was ^{14}C-dated using AMS at the National Ocean Sciences Accelerator Mass Spectrometry (NOSAMS) facility, Woods Hole, Massachusetts and the other was dated by U/Th using inductively-coupled plasma mass spectrometry (ICP-MS). Two radiocarbon dates and two U/Th dates were highly unrealistic when compared with the other dates from the same coral and were indicative of contamination or diagenesis; these four samples were, therefore, excluded from the reconstructions of ΔR.

^{14}C ages are typically reported as age-ranges corresponding to the 95% CI. In the following analysis, however, we used the most-probable-age estimate rather than the confidence interval. Treating the U/Th age as the true age[58], we used the U/Th age from each coral to obtain the expected radiocarbon age of that sample from the global marine calibration curve[57,62]. The

differences between the measured and expected radiocarbon yielded ΔR, the deviation from the global reservoir correction of ~400 years[57].

The error for each estimate of ΔR was calculated using the combined errors of the radiocarbon ages and expected radiocarbon ages from the marine calibration curve. The combined errors were calculated according to the following equation:

$$SE_{diff}=[(SE_1)^2+(SE_2)^2]^{0.5} \quad [5]$$

This equation uses the standard error for each date to determine the standard error of the difference between the dates, SE_{diff}.

Age-model

To develop a robust age-model for core EP09-28, we dated 15 corals throughout the core using U/Th analysis by ICP-MS. All dates are shown in Supplementary Table 4. Two dates were incongruous with dates from adjacent intervals (shown in red in Supplementary Table 4) and were removed from the age-model. The final U/Th age-model, used to interpolate ages for all the geochemical data, is shown in Supplementary Fig. 7.

Supplementary Tables

Supplementary Table 1. Standard deviations of geochemical ratios among replicate samples taken from individual corals. *n*=5 for the stable-isotope analyses. For the trace-element analyses, *n*=4 for CL-4 and *n*=3 for CL-21.

Year	Coral ID	$\delta^{18}O$	$\delta^{13}C$	Sr/Ca	Ba/Ca	B/Ca
2008	CL-4	0.38	0.20	0.10	0.08	0.03
2008	CL-15	0.13	0.11	-	-	-
2009	CL-12	0.23	0.18	-	-	-
2009	CL-21	0.19	0.20	0.03	0.07	0.03
Average		**0.23**	**0.17**	**0.06**	**0.08**	**0.03**

Supplementary Table 2. Standard deviations of geochemical ratios among multiple corals within two years: 2008 (*n*=11) and 2009 (*n*=10).

Year	$\delta^{18}O$	$\delta^{13}C$	Sr/Ca	Ba/Ca	B/Ca
2008	0.50	0.54	0.10	0.34	0.04
2009	0.74	0.35	0.08	0.27	0.04
Average	**0.62**	**0.45**	**0.09**	**0.30**	**0.04**

Supplementary Table 3. Ranges of the geochemical ratios from the raw data and the 200-yr running means of the raw data in comparison to the range of the 95% CI.

	Average range of 95% CI	Range in raw data	Range in 200-yr running mean
Sr/Ca	0.23	1.18	0.62
$\delta^{18}O$	0.97	2.72	1.40
$\delta^{18}O_{sw}$	1.64	8.81	2.67
Ba/Ca	1.56	9.42	3.47
$\delta^{13}C$	0.94	4.08	1.77
B/Ca	0.88	2.85	0.46

Supplementary Table 4. U/Th ages in years before present (yr BP; where present is 1950 C.E.) used to create an age-model for core EP09-28 from Contadora Island. All errors are reported as 2σ. $\delta^{234}U_{measured} = ([^{234}U/^{238}U]_{activity} - 1) * 1000$. $\delta^{234}U_{initial}$ was calculated based on ^{230}Th age (Th), i.e., $\delta^{234}U_{initial} = \delta^{234}U_{measured} * e^{\lambda 234T}$. Corrected ^{230}Th ages assume the initial $^{230}Th/^{232}Th$ atomic ratio of $4.4 \pm 2.2 \times 10^{-6}$. Those are the values for a material at secular equilibrium, with the bulk-earth $^{232}Th/^{238}U$ value of 3.8. Dates in red were excluded from the age-model.

Sample no.	Depth in core (cm)	$[^{238}U]$ (ppb)	$[^{232}Th]$ (ppt)	$^{230}Th/^{232}Th$ (atomic*10^{-6})	$\delta^{234}U$ (measured)	$^{230}Th/^{238}U$ (activity)	^{230}Th age (yr) (uncorrected)	^{230}Th age (yr) (corrected)	$\delta^{234}U_{initial}$ (corrected)	**^{230}Th age (yr BP) (corrected)**
C-49	33	2435±3	1493±30	1493±30	146.0±1.5	0.0065±0.0001	619±10	603±15	146±1	**540±15**
C-40	42.5	2330±2	39±4	8916±1006	144.8±1.4	0.0089±0.0001	855±11	855±11	145±1	**793±11**
C-24	61	3044±4	633±13	918±19	145.2±1.6	0.0116±0.0001	1107±6	1102±7	146±2	**1039±7**
C-53	76	2366±2	54±5	11049±1011	144.6±1.5	0.0152±0.0001	1454±13	1454±13	145±1	**1392±13**
C-56[1]	98	2252±3	354±9	4910±131	142.7±2.1	0.0469±0.0002	4563±22	4559±22	145±2	**4497±22**
C-124	99.5	2840±3	2525±51	742±15	144.2±1.6	0.0400±0.0002	3878±16	3856±22	146±2	**3793±22**
C-62	107	2137±2	70±7	23176±2321	143.2±1.7	0.0460±0.0002	4475±23	4474±23	145±2	**4412±23**
C-77	125	2312±2	84±6	21767±1557	142.0±1.6	0.0479±0.0002	4670±21	4669±21	144±2	**4607±21**
C-91	144	2543±7	317±8	6339±173	141.8±2.8	0.0480±0.0003	4678±33	4675±34	144±3	**4613±34**
C-101[2]	171	2568±6	123±5	17852±784	142.6±2.2	0.0520±0.0003	5075±33	5074±33	145±2	**5012±33**
C-101	171	2730±3	2604±52	880±18	144.2±1.6	0.0509±0.0001	4957±15	4933±23	146±2	**4870±23**
C-106	181	3046±3	668±15	3904±84	144.8±1.3	0.0506±0.0002	4925±17	4920±18	147±1	**4857±18**
C-118	204	2781±3	1531±31	1537±31	144.2±1.7	0.0513±0.0001	5000±16	4986±19	146±2	**4923±19**
785a	205	2595±3	541±11	4186±88	144.4±1.9	0.0530±0.0002	5161±26	5156±27	146±2	**5096±27**
C-11	230	2644±3	229±6	10092±273	144.7±1.7	0.0531±0.0001	5174±17	5171±17	147±2	**5109±17**
835a	253	2326±6	585±13	4553±99	142.2±2.3	0.0694±0.0003	6829±35	6823±35	145±2	**6761±35**

[1]Diagenetic screening showed this sample to contain precipitates of secondary aragonite.

[2]This sample gave ages incongruous with the other dates in the age-model. Re-analysis of the sample yielded the more realistic age of 4870±23, which was used in the final age-model.

Supplementary Figures

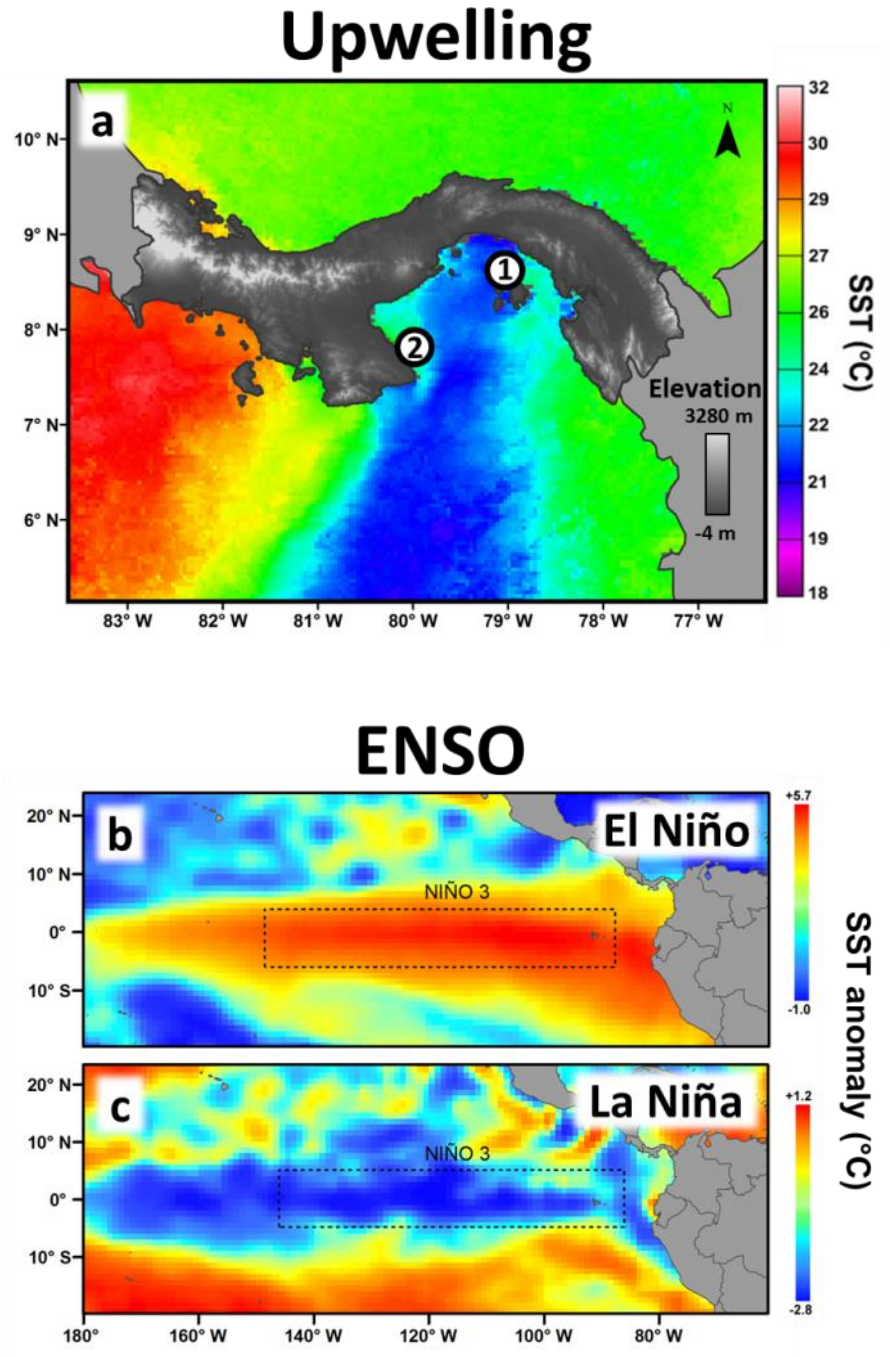

Supplementary Figure 1. (**a**) Sea-surface temperature (SST) in the TEP at the peaks of the 2009 upwelling season, and SST anomalies during (**b**) the El Niño in 1997 and (**c**) the La Niña in 1999. The numbers in (**a**) indicate (1) Contadora Island, our primary study location and (2) Iguana Island, where we collected additional measurements of ΔR. Images were created from MODIS/Aqua SST data using NASA's POET software (http://podaac-tools.jpl.nasa.gov/las).

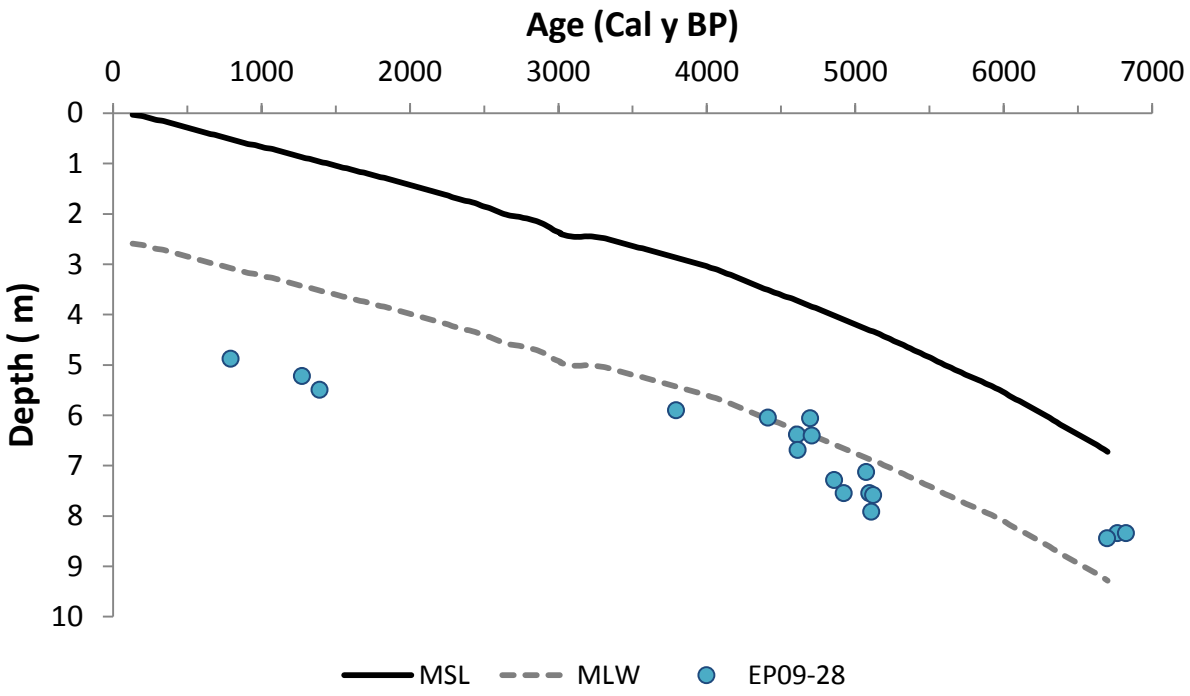

Supplementary Figure 2. Relationship of the depths of dated samples in our core (relative to mean sea level, or MSL) to the Holocene sea-level curve for the Caribbean (ref. 46; black line) and the putative sea level at low tide (dashed grey line; mean low water, or MLW, given that the average tidal range in the Gulf of Panamá is ~5.1 m).

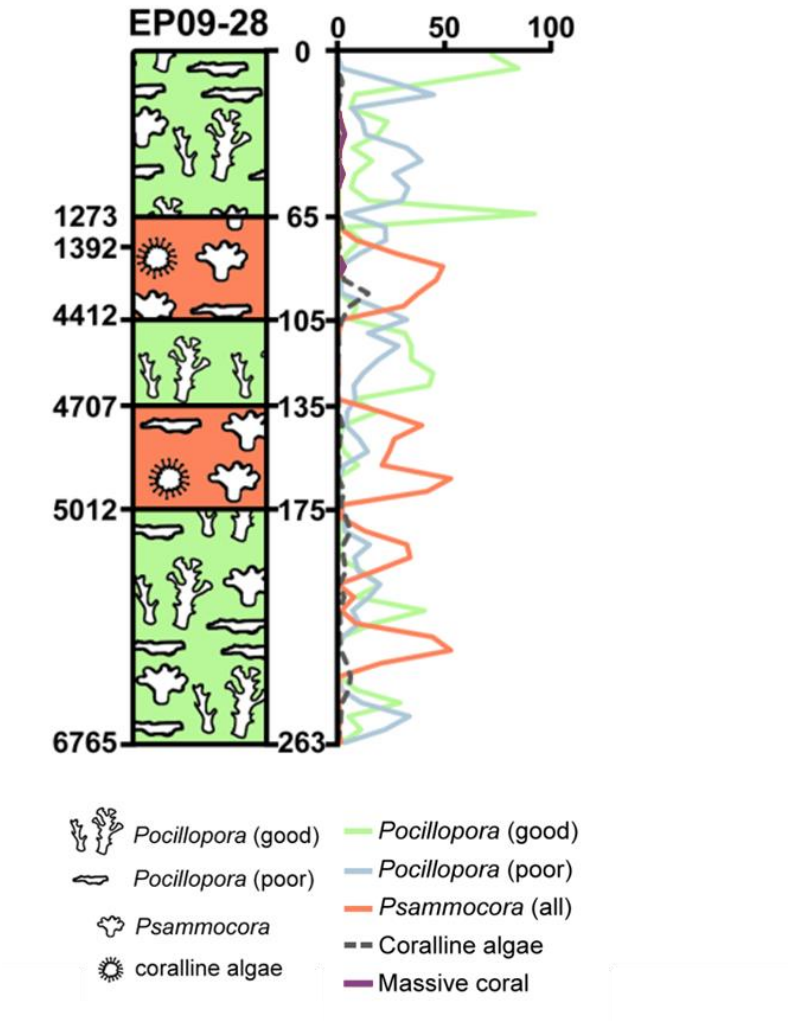

Supplementary Figure 3. Core-log showing the composition of EP09-28. The core-log is displayed by depth in cm (secondary y-axis), with ages of layers within the core in cal BP given on the primary y-axis. The core is aligned with graphical representations of the abundances of core constituents by mass in grams (x-axis). Fill colors in the core-log represent the dominant composition of the layers. Green represents *Pocillopora* spp. in good and intermediate taphonomic condition; blue represents *Pocillopora* spp. in poor taphonomic condition; pink represents *Psammocora stellata*; gray represents branching coralline algae; and yellow represents massive corals including *Porites* spp., *Pavona* spp., and *Gardineroseris planulata*.

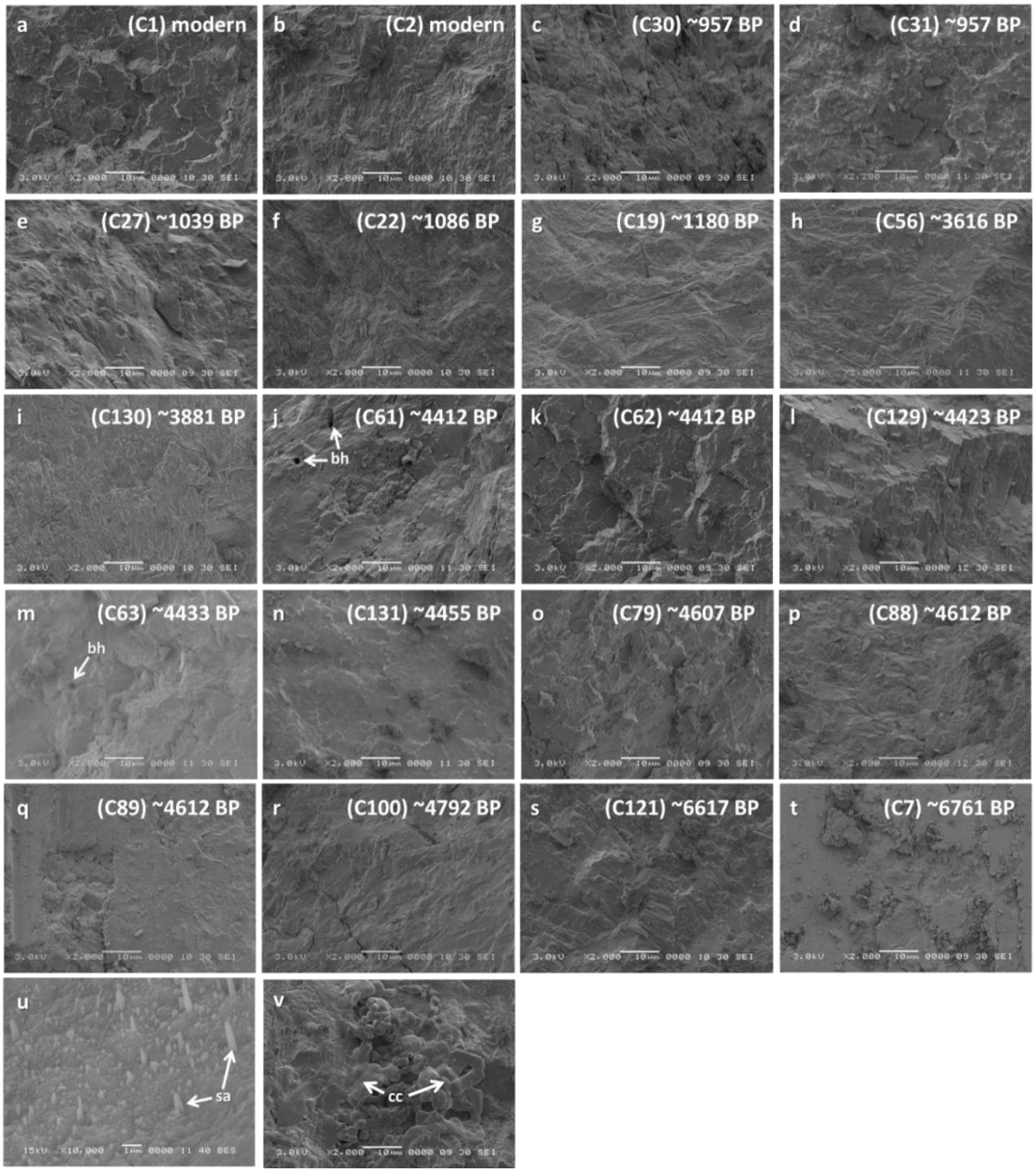

Supplementary Figure 4. Representative scanning electron microscope (SEM) images of the 20 coral skeletons screened for diagenetic alteration (**a**–**v**). The sample number (in parentheses) and approximate U/Th age of each coral is given in the top-right corner of each image. Each of these skeletons was mainly composed of primary aragonitic calcium carbonate but did contain some small boreholes (bh). The pristine skeletons in these images contrast with small portions of some of the coral skeletons in **u** and **v**; those portions of the skeletons were not sampled for geochemical analysis. The material in u and v contained secondary aragonite (sa) and calcite cements (cc), respectively. All samples were imaged at 2000x magnification with electron acceleration 5 kV and a spot-size of 30 mm. We also took an image of one coral, u, using the SEM's backscatter setting to better visualize the secondary aragonite crystals present in the skeleton.

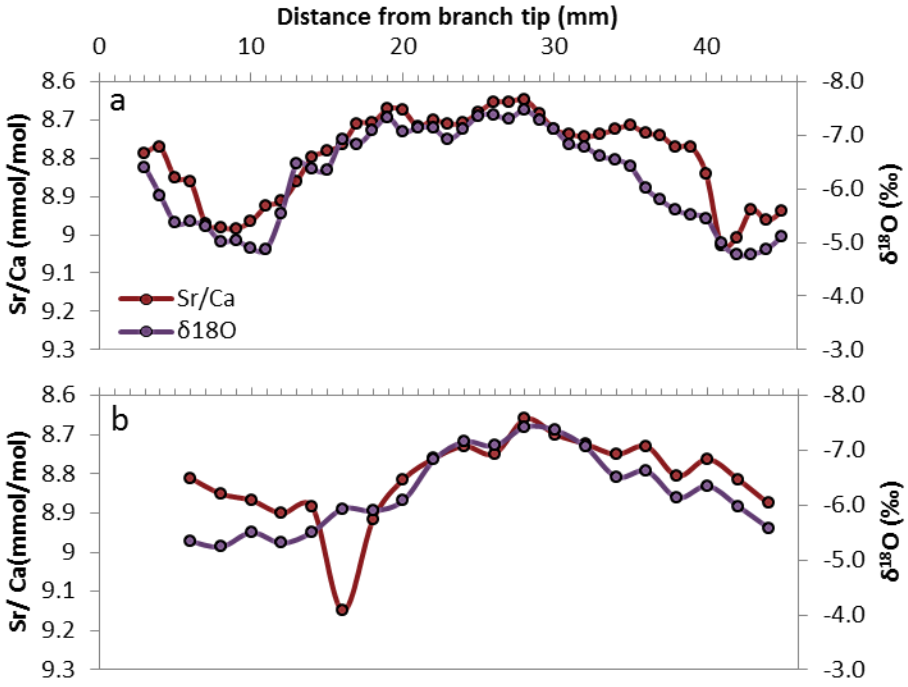

Supplementary Figure 5. Geochemical profiles of modern coral fragments (**a**) CL-1 and (**b**) CL-2 collected at Contadora Island in the Summer of 2011.

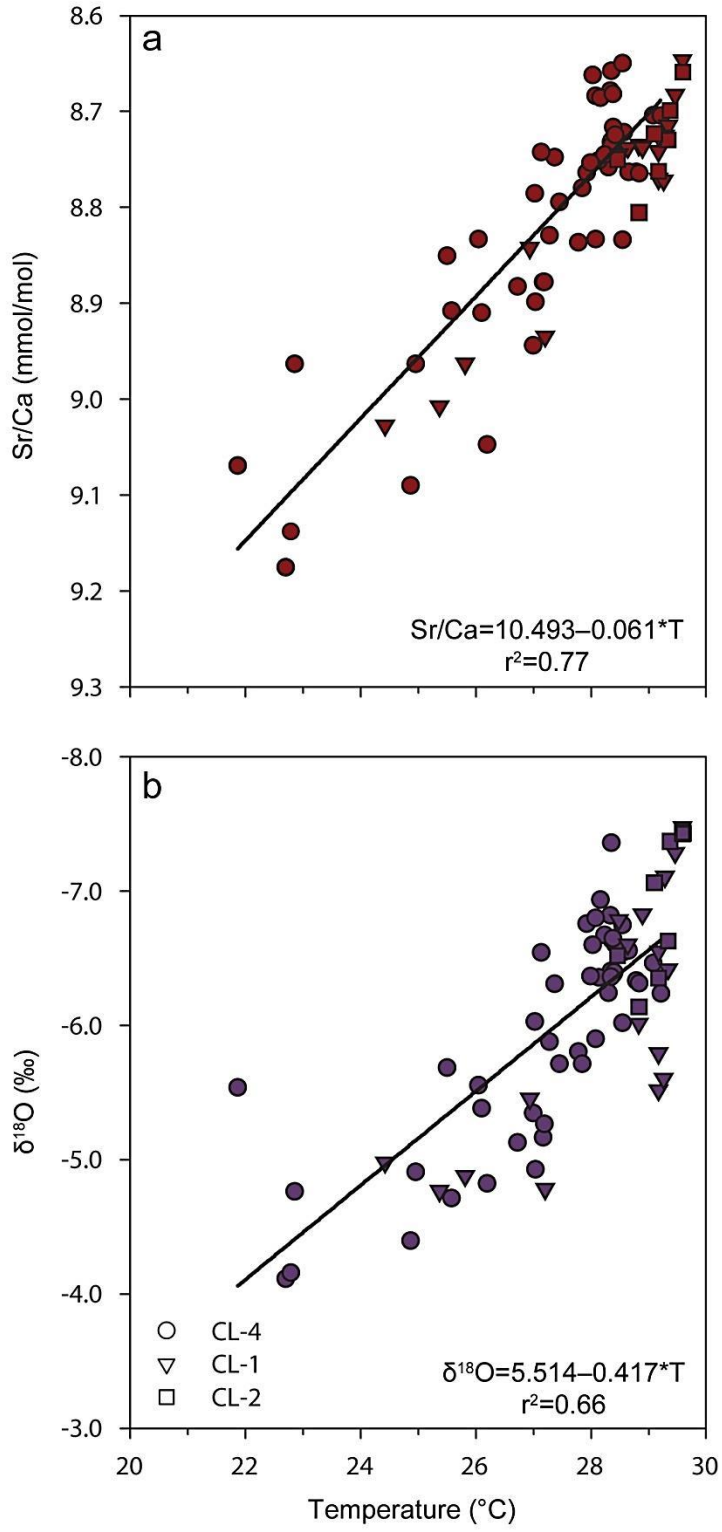

Supplementary Figure 6. Relationships between *in situ* temperature and (**a**) Sr/Ca and (**b**) $\delta^{18}O$ in three modern *P. damicornis* corals (CL-4, CL-1, and CL-2).

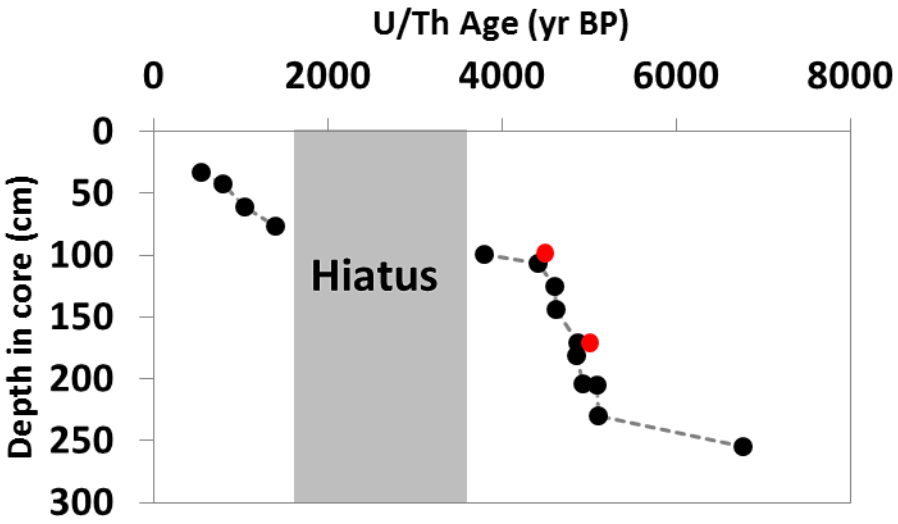

Supplementary Figure 7. U/Th age-model for core EP09-28 from Contadora. Points are U/Th dates from Supplementary Table 1. The two points in red were removed from the final age-model.

Literature Cited

30. Poveda, G., P. R. Waylen, and R. S. Pulwarty. Annual and inter-annual variability of the present climate in northern South America and southern Mesoamerica. *Palaeogeogr Palaeoclimatol Palaeoecol* **234**:3–27 (2006).
31. Glynn, P. W. and J. L. Maté. Field guide to the Pacific coral reefs of Panamá. *Proc 8th Int Coral Reef Symp* **1**:145–166 (1997).
32. D'Croz, L. and A. O'Dea. Variability in upwelling along the Pacific shelf of Panama and implications for the distribution of nutrients and chlorophyll. *Estuar Coast Shelf Sci* **73**:325–340 (2007).
33. Jiménez, C. and J. Cortés. Growth of seven species of scleractinian corals in an upwelling environment of the eastern Pacific (Golfo de Papagayo, Costa Rica). *Bull Mar Sci* **72**:187–198 (2003).
34. Glynn, P. W. and R. H. Stewart. Distribution of coral reefs in the Pearl Islands (Gulf of Panamá) in relation to thermal conditions. *Limnol Oceanogr* **18**:367–1379 (1973).
35. Glynn, P. W. Coral reef bleaching: ecological perspectives. *Coral Reefs* **12**:1–17 (1993).
36. Estoque, M. A., J. Luque, M. Chandeck-Monteza, and J. Gracia. Effects of El Niño on Panama rainfall. *Geofis Int* **24**:355–381 (1985).
37. Dai, A. and T. M. L. Wigley. Global Patterns of ENSO-induced precipitation. *Geophys Res Lett* **27**:1283–1286 (2012).
38. Lachniet, M. S. *et al*. A 1500-year El Niño/Southern Oscillation and rainfall history for the Isthmus of Panama from speleothem calcite. *J Geophys Res* **109**:D20117 (2004).
39. Glynn, P. W., J. L. Maté, A. C. Baker, and M. O. Calderón. Coral bleaching and mortality in Panama and Ecuador during the 1997–1998 El Niño-Southern Oscillation event: spatial/temporal patterns and comparisons with the 1982–11983 event. *Bull Mar Sci* **69**:79–109 (2001).
40. Pennington, J. T., K. L. Mahoney, V. S. Kuwahara, D. D. Kolber, R. Calienes, and F. P. Chavez. Primary production in the eastern tropical Pacific: a review. Progress in Oceanography **69**:285–317 (2006).
41. Glynn, P. W. Some physical and biological determinants of coral community structure in the eastern Pacific. *Ecol Monogr* **46**:431–456 (1976).
42. Eakin, C. M. and P. W. Glynn. Low tidal exposures and reef mortalities in the eastern Pacific. *Coral Reefs* **15**:120 (1996).
43. Kleypas, J. A., J. W. McManus, and L. A. B. Meñez. Environmental limits to coral reef development: where do we draw the line? *Am Zool* **39**:146–159 (1999).
44. Alexander, M. A., H. Seo, S. P. Xie, and J. D. Stott. ENSO's impact on the gap wind regions of the eastern tropical Pacific ocean. *J Clim* **25**:3549–3565 (2012).
45. Toscano, M. A., and I. G. Macintyre. Corrected western Atlantic sea-level curve for the last 11,000 years based on calibrated 14C dates from *Acropora palmata* framework and intertidal mangrove peat. Coral Reefs **22**:257-270 (2003).
46. Hopley, D., S. G. Smithers, and K. E. Parnell. The Geomorphology of the Great Barrier Reef: Development, Diversity, and Change. Cambridge University Press, Cambridge (2007).
47. Woodroffe, S. A. 2009. Testing models of mid to late Holocene sea-level change, North Queensland, Australia. *Quat Sci Rev* **28**:2474–2488.
48. Sayani, H. R. *et al*. Effects of diagenesis on paleoclimate reconstructions from modern and young fossil corals. *Geochim Cosmochim Acta* **75**:6361–6373 (2011).

49. Toth, L. T. Holocene coral reef development in the tropical eastern Pacific. Dissertation. Florida Institute of Technology, Melbourne, FL (2013).
50. Smith, S. V., R. W. Buddemeier, R. C. Redalje, and J. E. Houck. Strontium-calcium thermometry in coral skeletons. *Science* **204**:404–407 (1979).
51. Dunbar, R. B. and G. M. Wellington. Stable isotopes in a branching coral monitor seasonal temperature variation. *Nature* **293**:453–455 (1981).
52. Weil, S. M., R. W. Buddemeier, S. V. Smith, and P. M. Kroopnick. The stable isotopic composition of coral skeletons: control by environmental variables. *Geochim Cosmochim Acta* **45**:1147–1153 (1981).
53. Achim Z. and G. Grothendieck. zoo: S3 Infrastructure for Regular and Irregular Time Series. *J Stat Softw* **14**:1–27. URL http://www.jstatsoft.org/v14/i06/48. RStudio (2005).
54. R Core Team. R: A language and environment for statistical computing. R Foundation for Statistical Computing. Vienna, Austria. http://www.R-project.org/ (2013).
55. RStudio: Integrated development environment for R (Version 3.0.2). Boston, MA. http://www.rstudio.org/ (2013)
56. Stuiver, M. and H. A. Polach. Discussion: reporting of ^{14}C data. Radiocarbon **19**:355–363 (1977).
57. Reimer, P. J. and R. W. Reimer. A marine reservoir correction database and on-line interface. *Radiocarbon* **43**:461–463 (2001).
58. Bard, E., M. Arnold, R. G. Fairbanks, and B. Hamelin. ^{230}Th-^{234}U and ^{14}C ages obtained by mass spectrometry on corals. *Radiocarbon* **35**:191–199 (1993).
59. Fontugne, M., M. Carré, I. Bentaleb, M. Julien, and D. Lavallée. Radiocarbon reservoir age variations in the South Peruvian Upwelling during the Holocene. *Radiocarbon* **46**:531–537 (2004).
60. Soares, A. M. M. and J. M. A. Dias. Coastal upwelling and radiocarbon—evidence for temporal fluctuations in ocean reservoir effect off Portugal during the Holocene. *Radiocarbon* **48**:45–60 (2006).
61. Zaunbrecher, L.K., K.M. Cobb, J.W. Beck, C.D. Charles, E.R.M. Druffel, R.G. Fairbanks, S. Griffin, and H. Sayani. Coral records of central tropical Pacific radiocarbon variability during the last millennium. *Paleoceanography* 25:PA4212 (2010)
62. Reimer, P. J. *et al*. IntCal09 and Marine09 radiocarbon age calibration curves: 0–50,000 years cal BP. *Radiocarbon* **51**:1111–1150 (2009).